Available online at www.sciencedirect.com
SCIENCE DIRECT
Physics and Chemistry of the Earth 31 (2006) 143–153
PHYSICS and CHEMISTRY of the EARTH
www.elsevier.com/locate/pce

The physical nature of thermal anomalies observed before strong earthquakes

S.A. Pulinets [a,*], D. Ouzounov [b], A.V. Karelin [c], K.A. Boyarchuk [c], L.A. Pokhmelnykh [d]

[a] *Institute of Geophysics, UNAM, Mexico City, Mexico*
[b] *NASA Goddard Space Flight Center/SSAI, Greenbelt, Maryland, USA*
[c] *IZMIRAN, Russian Academy of Sciences, Troitsk, Russia*
[d] *ELAT Company, Mexico City, Mexico*

Accepted 6 February 2006
Available online 24 May 2006

Abstract

The paper examines the effect of air ionization on the thermal balance of the boundary layer of atmosphere. In seismically active areas the increased radon emanation from active faults and cracks before earthquakes is the primary source of air ionization. The problem is analyzed both on microscopic and macroscopic levels and in both cases the significant changes of the air relative humidity and air temperature are obtained. This happens due to the water molecules attachment to the newly formed ions (or in other words, condensation) which leads to the excretion of the latent heat. Obtained results permit us to explain the changes of the surface temperature and the surface latent heat flux increase before earthquakes observed by remote sensing satellites, as well as ground based measurements of the air temperature and relative humidity variations before the Colima earthquake (M7.6) of 2003 in Mexico, Hector Mine earthquake (M7.1) of 1999 in USA and Parkfield earthquake (M6) of 2004 in USA. These findings are also supported by the results of active experiments where the installation of artificial ionization of atmosphere is used.

Keywords: Air ionization; Radon; Latent heat; Thermal anomaly; Earthquake

1. Introduction

Thermal anomalies observed within the area of earthquake preparation a few days before the seismic shock (Tronin, 1999; Tramutoli et al., 2001; Tronin et al., 2004) usually were interpreted as the thermal flux deposited from the earth's crust in seismically active areas (Ouzounov and Freund, 2004). But discovered recently by Dey and Singh (2003) anomalous variations of the surface latent heat flux (SLHF) before earthquakes, involve the variations of air humidity which cannot be explained by the heat deposit from the crust and requires other interpretation. One can find the methodology of the latent heat estimation from remote sensing data in Schulz et al. (1997). At the same time the IR sensors used by remote sensing satellites, can register the changes of air temperature also as a part of the SLHF variations. The ambiguity of situation was resolved by the developed model of seismo-ionospheric coupling (Pulinets and Boyarchuk, 2004). The part of the model describing the generation of anomalous electric field in the zones of earthquake preparation involves the process of formation of gaseous aerosols with water molecules attachment, which is essentially connected with the latent heat variations. During these processes the large amount of heat (~800–900 cal/g) is released or consumed (Sedunov et al., 1997). Similar processes take place under action of cosmic rays on the atmosphere. Air ionization provided by cosmic rays results in formation of aerosols as condensation nuclei for clouds (Yu and Turco, 2001; Timofeev et al., 2003). In normal conditions when the number of

* Corresponding author. Tel.: +52 55 56224139; fax: +52 55 555502486.
E-mail address: pulse@geofisica.unam.mx (S.A. Pulinets).

1474-7065/$ - see front matter © 2006 Elsevier Ltd. All rights reserved.
doi:10.1016/j.pce.2006.02.042

large ionized ion clusters is small, the meteorological processes prevail. But when the concentration of hydrated particles created by radon ionization increases up to values 10^5–10^6 cm^{-3} (Pulinets and Boyarchuk, 2004) they provide an essential contribution in the SLHF variations up to anomalous values registered by satellites. The purpose of the present paper is to model the above mentioned processes and to compare with experimental measurements around the time of recent major earthquakes, as well as with the results of active experiments using the special equipment for artificial ionization of the atmosphere.

2. Long-term thermal effects associated with seismic activity

Mil'kis (1986) demonstrated the presence of thermal anomalies during the month (or season) of the strong earthquakes in the former Soviet Union. He used the data from more than 120 meteorological stations in Turkmenia, Uzbekistan and other regions of Central Asia. Using the assemblage of climatic elements (data from the meteorological stations in Turkmenia and Uzbekistan) their anomalous variations were studied around the time of the following earthquakes: Ashkhabad October 5, 1948 ($M = 7.3$); Gazly April 8 ($M = 7$), May 17 ($M = 7.2$) 1976; and March 20, 1984 ($M = 7$). Individual climatic parameters were studied also for the following earthquakes: Krasnovodsk July 8, 1895 ($M = 8.2$); Sarez February 18, 1911 ($M = 7.4$); Germab May 1, 1929 ($M = 7.2$); Kemine-Chuy June 20, 1938 ($M = 6.9$); Garm April 20, 1941 ($M = 6.4$); Chatkal November 2, 1946 ($M = 7.5$); Kazandzhik November 4, 1946 ($M = 7.0$); Tashkent April 26, 1966 ($M = 5.6$); Ashkhabad November 15, 1968 ($M = 5.6$); and Vyshko-Burun February 22, 1984 ($M = 6.0$). Fig. 1 presents his results of air temperature measurements (mean monthly temperature for long-term intervals – several tens of years). In every case the month when earthquake takes place is selected for analysis. It means that if an earthquake took place in January, the mean January temperature for several tens of years is monitored. One can see that within interval of tens of years the mean monthly temperature for the year of earthquake practically in all cases is anomalously high and is the local maximum for the multi-year interval.

The same long-term behavior of the mean monthly temperature was observed for the Colima earthquake in Mexico on 23 of January 2003 ($M = 7.8$). Fig. 2 demonstrates the 50-years interval of January mean monthly temperature at Manzanillo meteorological station (closest to the earthquake epicenter), and for year 2003 one can observe the absolute maximum of the temperature for the whole interval of presented records.

3. Short-term thermal effects

We analyzed the meteorological data around the time of Hector Mine earthquake M7.1 16 October 1999, USA, Colima earthquake M7.6 21 January 2003, Mexico, and Parkfield earthquake M6 28 September 2004, USA. More detailed information was collected for Colima earthquake. Data of three meteorological stations (air temperature and relative humidity) are presented in Fig. 3. Colima and Manzanillo stations are situated at a similar distance of the epicenter (60 and 55 km, respectively according to USGC location). And the third station (Cuernavaca) is near 900 km from the epicenter. One can easily see the difference. The first two stations (Fig. 3a and b) clearly show the sharp drop of relative humidity one week before the seismic shock, and no effect is observed at the third station (Fig. 3c). Taking into account that Manzanillo is at the ocean shore, the humidity of order of 40% at tropics is very unusual. We can mark also the absolute monthly minimum of air temperature at Colima Station on 13 of January, and temperature maxima at both stations on 14 and 15 of January. Relative humidity minimum at Colima coincides with the absolute monthly maximum at the same day of 14 January. The map of the surface air temperature distribution over Mexico for 1400 LT on 14 of January 2003 is shown in Fig. 4. The most remarkable feature of this distribution is the local temperature maximum close to the epicenter position of impending earthquake, and the temperature increase stretched along the coast in accordance with the subduction trench orientation.

The local time variations of the air temperature and relative humidity somehow mask the main effect connected with the radon variations and consequent changes of the atmosphere parameters. Therefore, we used the special parameter which reflects both the temperature and humidity variations, namely the daily temperature range – the difference between the daily temperature maximum and minimum. Variations of this parameter related to the earthquake moment is presented in Fig. 5a. One can see the local minimum 9 days before the earthquake what corresponds to the local maximum of the relative humidity, then the absolute maximum of the range which corresponds to the relative humidity minimum, and then the gradual drop of the temperature range up to the earthquake occurrence.

The presence of similar temperature variations was checked for the periods around the time of Hector Mine earthquake M7 (16 October 1999) and Parkfield earthquake in California M6 (28 September 2004). Same daily temperature range variations for two meteorological stations in the vicinity of Hector Mine earthquake epicenter (Borrego station) and in the vicinity of Parkfield earthquake (Paso Robles station) are shown in Fig. 5b and c, respectively. It is interesting to mark that the time intervals for characteristic points of range variations (dashed lines) for Colima earthquake and Hector Mine earthquake are identical.

Not occasional character of atmosphere parameters variations before earthquakes was confirmed recently by the satellite remote sensing measurements. Ouzounov et al. (2005) and Ouzounov et al. (2006) using the measurements of AVHRR instrument onboard the NOAA satellites demonstrated the temporal variations of ongoing longwave radiation (OLR) over the epicenters of strong earthquake at Taiwan M5.7, 12 February 2005, and catastrophic Suma-

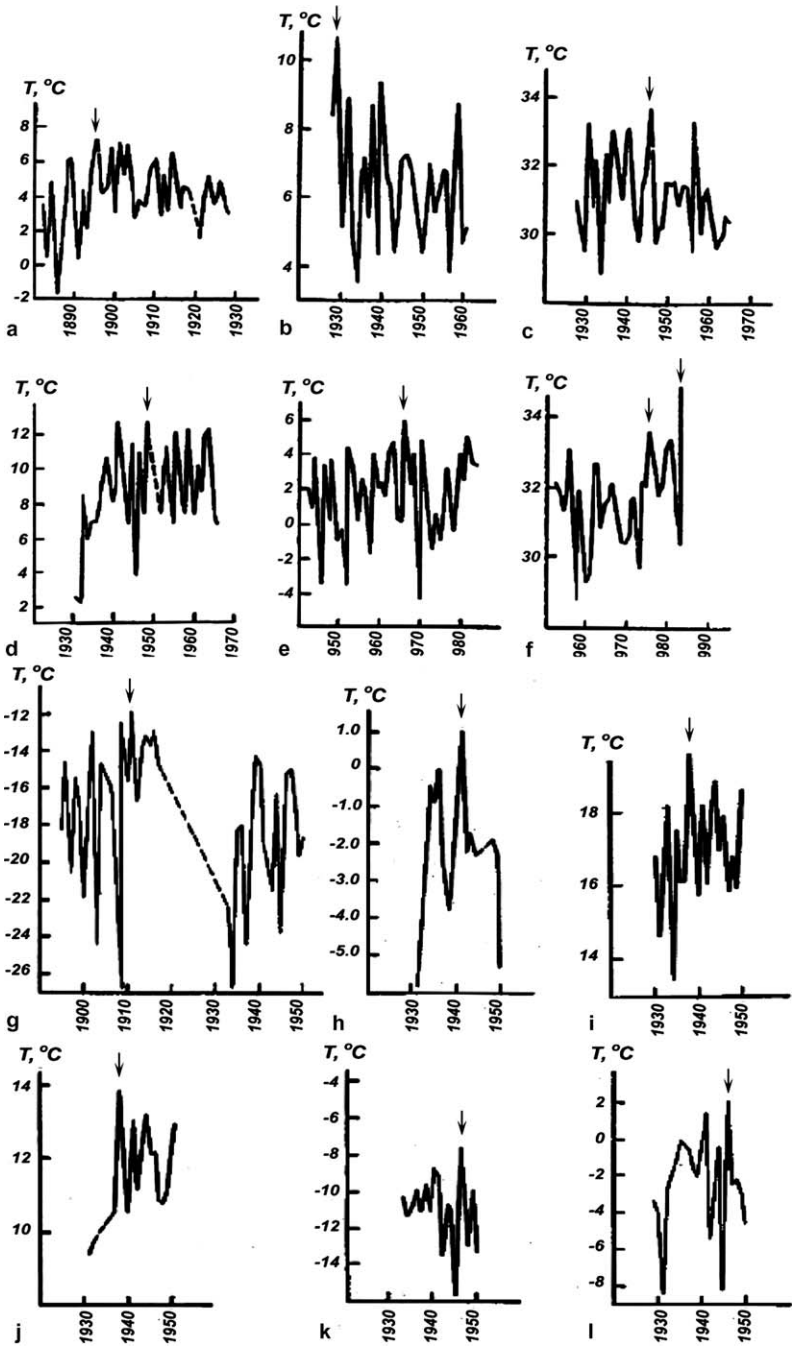

Fig. 1. The increases of air temperature in the multi-year regime (the abscissa indicating the year) for individual months and seasons of the year as precursor anomalies of strong earthquakes (data are from the meteorological stations nearest to the epicenter): (a) Krasnovodsk earthquake; (b) Germab earthquake; (c) Kazandzhik earthquake; (d) Ashkhabad 1948 earthquake; (e) Tashkent earthquake; (f) Gazly 1976 and 1984 earthquakes; (g) Sarez earthquake; (h) Garm earthquake; (i, j) Kemine-Chuy earthquake, average monthly temperature in May at the Tokmak meteorological station (i) and the Novorossiyka station (j); (k, l) Chatkal average monthly temperatures for February at the Chatkal (k) and the Toe River Mouth (l) meteorological stations. (After Mil'kis, 1986).

tra earthquake M9, 26 December 2004. Variations of the mean (averaged records for 4 NOAA satellites) value of this parameter are shown in Fig. 6. Presented variations demonstrate the striking similarity to the ground based records presented in Fig. 5 showing the same temporal pattern and time scale in relation to the earthquake moment.

Summarizing the obtained results on variations of the meteorological parameters around the time of strong ($M > 6$) earthquakes one can conclude that within the time interval two weeks before the seismic shock the essential variations of the air temperature are observed with increased range between the maximum and minimum daily temperatures. Within the same time interval the relative humidity drop is observed close to the epicenter of impending earthquake. The spatial scale of the thermal anomalies before strong earthquakes ($M > 6$) reaches several

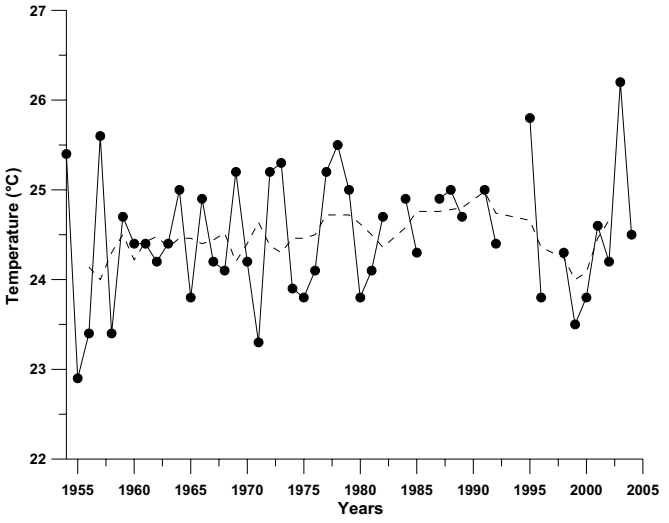

Fig. 2. January mean monthly temperature at Manzanillo station for the time interval 1954–2004.

hundreds km (the area is of order of 400 000 km^2), Mil'kis (1986). The month or season of the year when the strong earthquake happened is usually with anomalously high temperatures in comparison with other years within the time intervals of tens of years.

4. Physical mechanism

Looking from the perspective of the Lithosphere–Atmosphere–Ionosphere (LAI) model presented in Pulinets and Boyarchuk (2004), radon variations are the primary source of the atmosphere electricity changes a few days before the strong earthquakes. As it was demonstrated recently (Inan, 2005), radon variations before earthquake have similar time scale as the observed air temperature variations. The peak of radon emanation is reached 4–10 days before the seismic shock which happens on the falloff part of the observed local maximum of the radon variation. Zafrir et al. (2005) observed correlation of the radon variations and the air temperature. These results give us foundation to start calculations of the effects on the radon ionization on the air temperature and the relative humidity.

4.1. Macroscopic approach

In the thermal balance of the atmosphere (total heat budget is ~185 W/m^2) the latent heat of the water evaporation is very significant (~88 W/m^2). It means that changing of the latent heat balance essentially contributes to the air temperature variations. During water condensation on ions, the large number of the water molecules can be attached to the ion, it means that it grows up to some critical mass $m_{\max}$. The heat deposit w is equal to

$$w = m_{\max} U_0 \tag{1}$$

where U_0 is the latent heat of evaporation. If the ionization source produces the ions with the velocity $\mathrm{d}N/\mathrm{d}t$, the heat P_a deposited into the atmosphere can be expressed as (Pokhmelnykh, 2003):

$$P_a = w \cdot \mathrm{d}N/\mathrm{d}t \tag{2}$$

Each α-particle emitted by ^{222}Rn with the average energy $E_\alpha \approx 6$ MeV can produce theoretically about of 2×10^5 electron–ion pairs. The output of radon can reach 12 eman before an earthquake, which corresponds to the ionization rate about 7.6×10^3 cm^{-3} s^{-1}. It means that even minor increase of the radon emanation (usually, it is observed the increase by 20–30%) can lead to changes of the air temperature if this emanation takes place over the large territory of the earthquake preparation zone. Its radius is determined as (Dobrovolsky et al., 1979):

$$\rho = 10^{0.43M} \text{ km} \tag{3}$$

where M is the earthquake magnitude.

The high effectiveness of the air heating is explained by the fact that the energy necessary to the changes of air temperature is already stored in water vapor. Actually the large amount of solar energy spent for water evaporation is released and ionization only helps to release the latent heat of the water vapor by creation of the condensation centers in the form of ions. It is because of the fact that the hydration reactions are catalytic reactions in their nature. Using the artificial source of air ionization, it is possible to reach the gain (ratio of the energy spent for air ionization and released in the form of the latent heat) of order of 5×10^8 (Pokhmelnykh, 2003).

Taking into account that the ionization anomalies take place within the large areas of the earthquake preparation zone, the effects of the meteorological scale can be caused by comparatively small increase of the air ionization. Mil'kis (1986) demonstrates the thermal anomalies before strong earthquake in Central Asia within the areas of order of 400 000 km^2. These earlier results are supported now by the satellite remote sensing measurements demonstrating the large areas subjected to thermal anomalies before strong earthquakes (Tramutoli et al., 2001; Tronin et al., 2004; Ouzounov and Pulinets, 2005).

4.2. Microscopic approach

The problem of the latent heat release associated with air ionization can be divided into two parts: the problem of water condensation itself, and additional problem connected with the fact that water is condensed not on the water drop but on the molecular ion having the chemical potential different from the water molecule chemical potential. This fact changes the rate of evaporation/condensation. It means that for the same energy deposit the process of evaporation/condensation can be slower or

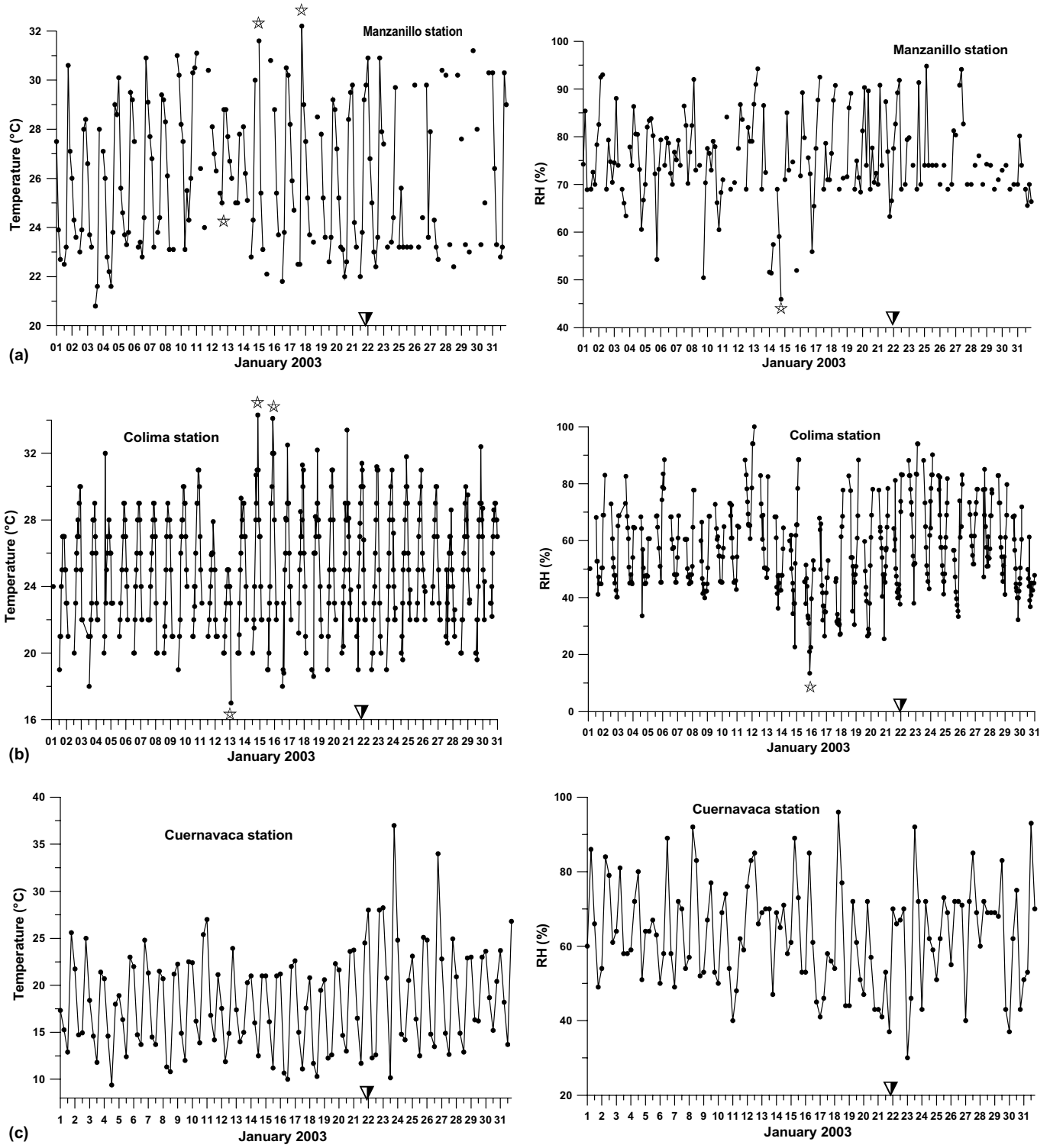

Fig. 3. January 2003 air temperature (left panel) and relative humidity (right panel) measured at three meteorological stations: (a) Manzanillo, (b) Colima, (c) Cuernavaca. (▼) indicates the earthquake moment, (☆) indicate the parameters peculiarities which interpret as precursors phenomena.

faster depending on the chemical potential, and consequently, the air humidity changes due to the changes of the chemical potential.

Dependence of the saturated water vapor concentration on the temperature can be derived from the Clausius–Clapeyron (Fermi, 1956) and Mendeleev–Clapeyron equations Yavorski and Detlaf (1996):

$$n = \frac{A}{T} \cdot \exp\left(-\frac{U}{k \cdot T}\right) \tag{4}$$

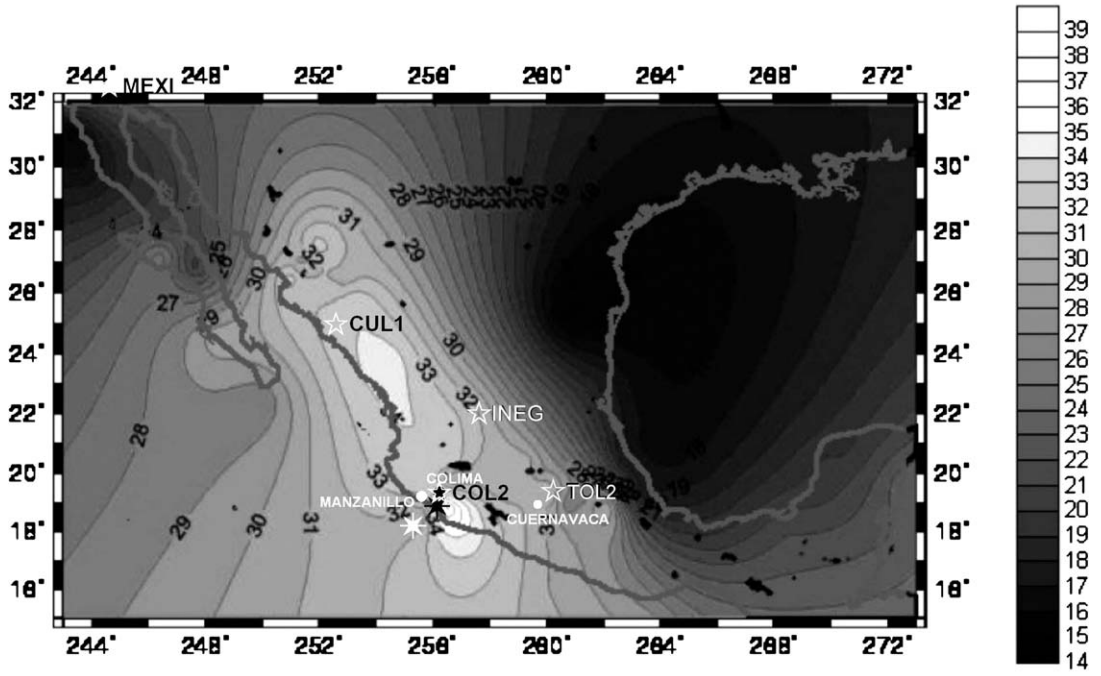

Fig. 4. The map of the surface air temperature at Mexico on 14 January 2003 at 1410 LT, reduced to the sea surface level. (☆) indicate positions of INEGI GPS receivers; (✷)-epicenter positions of the Colima earthquake determined by NSGS (white) and SSN (black); (●) show positions of meteorological stations at Manzanillo, Colima and Cuernavaca.

Here, k – Boltzman constant, U – latent heat of evaporation related to one molecule, A – constant. The evaporation latent heat related to one molecule (or in other words, the Gibbs chemical potential or work function) can be estimated from the evaporation heat $Q = 40.683$ kJ/mol under the boiling temperature $U_0 = Q/N_A = 0.422$ eV where $N_A = 6.022 \times 10^{23}$ 1/mol. This work function is equal to the energy of the dipole–dipole interaction of the rotating dipoles on the distance $r = 2.46$ Å which is the water molecule radius. Evaporation and condensation are the phase transitions of the first order. The phase transition happens under chemical potential equality. For the one-component system the chemical potential is equal to the thermodynamic potential related to the one particle. It means that the latent heat of evaporation U is equal to the chemical potential of the molecule in the water drop and can be calculated as (Zatsepina, 1998):

$$U = \frac{2 \cdot \mu^2 \cdot \mu^2}{3 \cdot k \cdot T \cdot r^6} \tag{5}$$

where $\mu = 1.85 \times 10^{-18}$ CGS cm – the dipole moment of the water molecule H_2O. The same work corresponds to the formation of the drop embryo (Green and Lane, 1964) with the critical radius $r = 4.76$ Å and surface tension $\gamma = 72.88$ dyn/cm.

$$W_{cr} = \frac{4}{3} \cdot \pi \cdot r_{cr}^2 \cdot \gamma \tag{6}$$

Just this demonstrates that the work function is equal to the dipole–dipole interaction energy. And here the second factor appears. The humid atmosphere under action of the solar radiation, cosmic rays, and other kinds of ionizing radiation as radon is not a one-component system. Under the action of radiation the new formed ions enter in the chain of plasmachemical reactions leading to the complex ion clusters formation. One can find the final ion composition under action of cosmic rays in Timofeev et al. (2003). Pulinets and Boyarchuk (2004) regarded the similar chain of reactions for the case of the air ionization by radon. Under action of radon ionization a large amount of O_2^+ ions is formed in atmosphere in the initial stage both as a result of direct ionization, and as a result of charge exchange between an initial ion N_2^+ and electrons, which fast adhere to atoms of oxygen, since the oxygen has a significant energy of affinity to electrons, forming the negative ions O^- and O_2^-. As a result of fast ion-molecular reactions during an interval of the order 10^{-7} s the main elementary tropospheric ions will be formed: O^-, O_2^-, NO_2^-, NO_2^-, CO_3^- and O_2^+, NO^+, H_3O^+. The concentration of electrons is so insignificant, that they can be neglected. The large amount of water vapor molecules contained in the troposphere ($\sim 10^{17}$ cm^{-3}), having a noticeable dipole moment $p = 1.87D$, leads to hydration of elementary ions and to the formation of ion complexes of type $NO_2^- \cdot (H_2O)_n$ and $NO_3^- \cdot (H_2O)_n$, $NO_3^- \cdot (HNO_3)_n(H_2O)_m$ and $O_2^+ \cdot (H_2O)$, $NO^+ \cdot (H_2O)_n$, $H^+ \cdot (H_2O)_m$ and $H_3O^+ \cdot (H_2O)_n$ which happens rather fast. It is estimated that the ion concentration in the area of earthquake preparation can reach 10^5–10^6 cm^{-3}, which essentially changes the electric properties of the near ground layer of atmosphere. These clusters

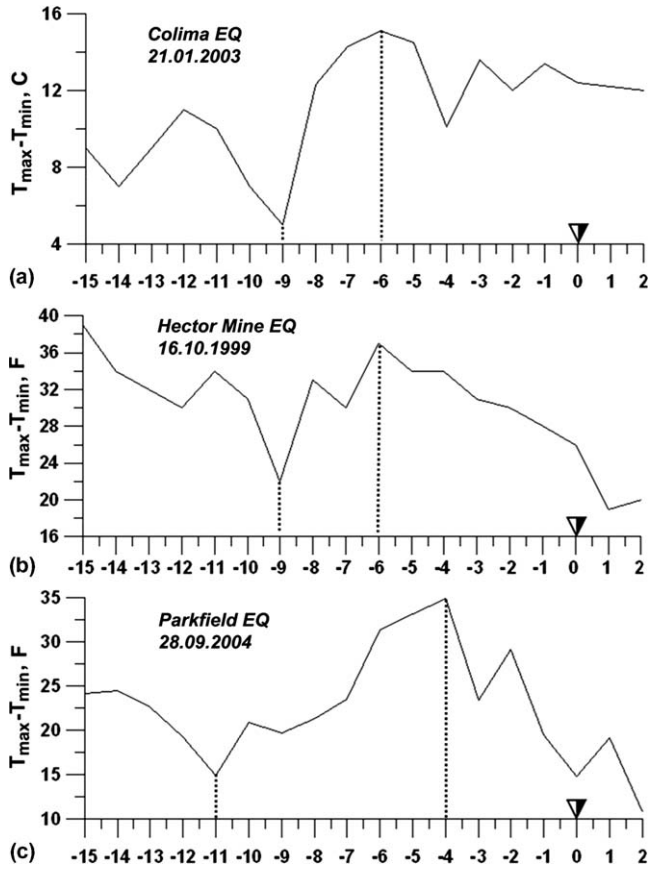

Fig. 5. Daily surface air temperature range variations registered close to the epicenters of strong earthquakes. From top to bottom: Colima earthquake M7.6 of 2003, (Mexico); Hector Mine earthquake M7.0 of 1999, (USA); Parkfield earthquake M6 of 2004, (USA). (▼) indicates the earthquake moment, (dashed lines) indicate the parameters peculiarities which we interpret as precursors phenomena.

become the centers of condensation but with other work function and other chemical potential. The changes of the chemical potential were taken into account in calculations of relative humidity. To facilitate calculations we still regard the system as one-component but with the changing chemical potential. Using the formulas (5) and (6) the changes of the chemical potential affecting the relative humidity can be calculated in the following form:

$$H(t) = \frac{\exp(-U(t)/k\cdot T)}{\exp(-U_0/k\cdot T)} = \exp\left(\frac{U_0 - U(t)}{k\cdot T}\right) = \exp\left(-\frac{0.032\cdot \Delta U\cdot \cos^2 t}{(k\cdot T)^2}\right) \quad (7)$$

where $U(t) = U_0 + \Delta U\cdot\cos^2 t$, ΔU – is the chemical potential correction averaged-by-the-volume as a result of external impact. The daily variations of the solar radiation were taken into account as cosine square. It is taken into account also that U_0 was calculated for the boiling temperature. The results of calculation for the case of the Colima earthquake are presented in Fig. 7 for three values of $\Delta U = 0.019$; 0.022 and 0.03 eV (from top to bottom). For a better visualization, the reversed value $1/H$ is shown. The blue line represents the inverse value of the experimentally measured relative humidity at Colima station, and the red line – inverse value of calculated relative humidity. One can see that during the period of observation the evaporation velocity changed significantly, which corresponds to the different values of ΔU. The changes of ΔU can be explained by the formation of a lot of centers of condensation in the form of complex clusters. In this case, the work function for the water molecules is determined as interaction of the charged cluster with the rotating dipole (Zatsepina, 1998):

$$U_{cd} = \frac{q^2\cdot\mu^2}{3\cdot k\cdot T\cdot r^4}, \quad (8)$$

where q is the dipole charge. The energy of the dipole-charge interaction on the distance $r_{cd} = 4.7$ Å is equal to $U_{cd} = 0.65$ eV.

Formation of the large clusters of the aerosol size under action of ionizing radiation was demonstrated in the laboratory experiment (Fig. 8) where in the gas chamber the thoron was injected periodically (Bricard et al., 1968).

The detailed calculations of the water vapor concentration in the air were made using the complete kinetic model of the air taking into account all the possible components NO, NO_2, NO_3, N_2O_5, N_2O, O, N, H, HO_2, H_2, OH, H_2O_2, HNO, HNO_2, HNO_3, HNO_4, C, CN; excited atoms and molecules: $O_2^*(^1\Delta)$, $O^*(^1D)$, $O^*(^1S)$, $N_2^*(A)$, $N^*(^2D)$; positive ions: N^+, N_2^+, N_3^+, N_4^+, O^+, O_2^+, O_4^+, O_6^+, O_8^+, H^+, H_2^+, H_3^+, NO^+, NO_2^+, NO_3^+, N_3O^+, $N_2O_2^+$, $N_2O_3^+$, H_2O^+, OH^+, H^+O_2, $H^+(H_2O)$, $O_2^+(H_2O)$, $H_2O^+(H_2O)$, $O_2^+(H_2O)_2$, $H^+(H_2O)_2$, $H^+(H_2O)_3$, $H^+(H_2O)_4$, $H^+(H_2O)_5$, $H^+(H_2O)_6$, $H^+(H_2O)_7$, $H^+(H_2O)_8$, $H^+(H_2O)O_2$, N_2H^+, $H^+(N_2O)$, $N^+(H_2O)$, $NO^+(H_2O)$, $NO_2^+(H_2O)$, $H^+(H_2O)N_2$, $NO^+(H_2O)_2$, $NO_2^+(H_2O)_2$, $NO^+(H_2O)_3$, $NO^+(H_2O)N_2$, $NO^+(H_2O)_2N_2$, C^+, CO^+, CO_2^+, $O^+(CO_2)$, $O_2^+(CO_2)$, $CO^+(CO)$, $CO^+(CO_2)$, $CO_2^+(CO_2)$, $O_2^+(CO_2)_2$, $CO^+(CO_2)CO$, $H^+(CO)$, $H^+(CO_2)$, $CO_2^+(H_2O)$, $NO^+(CO_2)$, $NO^+(H_2O)CO_2$, $NO^+(H_2O)_2CO_2$, $CO^+(H_2O)$, $H^+(CO)_2$; negative ions: O^-, O_2^-, O_3^-, NO_2^-, $O^-(NO_2)$, $O_2^-(H_2O)$, $O_3^-(H_2O)$, $O_2^-(H_2O)_2$, $NO_3^-(HNO_3)$, $NO_2^-(H_2O)$, $NO_3^-(H_2O)$, $NO_3^-(H_2O)HNO_3$, $NO_3^-(HNO_3)_2$, $O^-(CO_2)$, $O_2^-(CO_2)$, $O^-(CO_2)H_2O$ and electrons. The results of calculation are presented in Fig. 9 for three values of $\Delta U = 0.019$; 0.022 and 0.03 eV. One can see from the figure that the relative humidity can change significantly after several hours of action of ionizing source up to very low levels like 30%, and that it is accompanied automatically by the growth of the air temperature.

5. Practical applications using the meteorological data

It is possible to solve the reversed problem – using the meteorological data on the relative humidity and air temperature to calculate the changes of the chemical potential ΔU. Our calculations for the several recent important

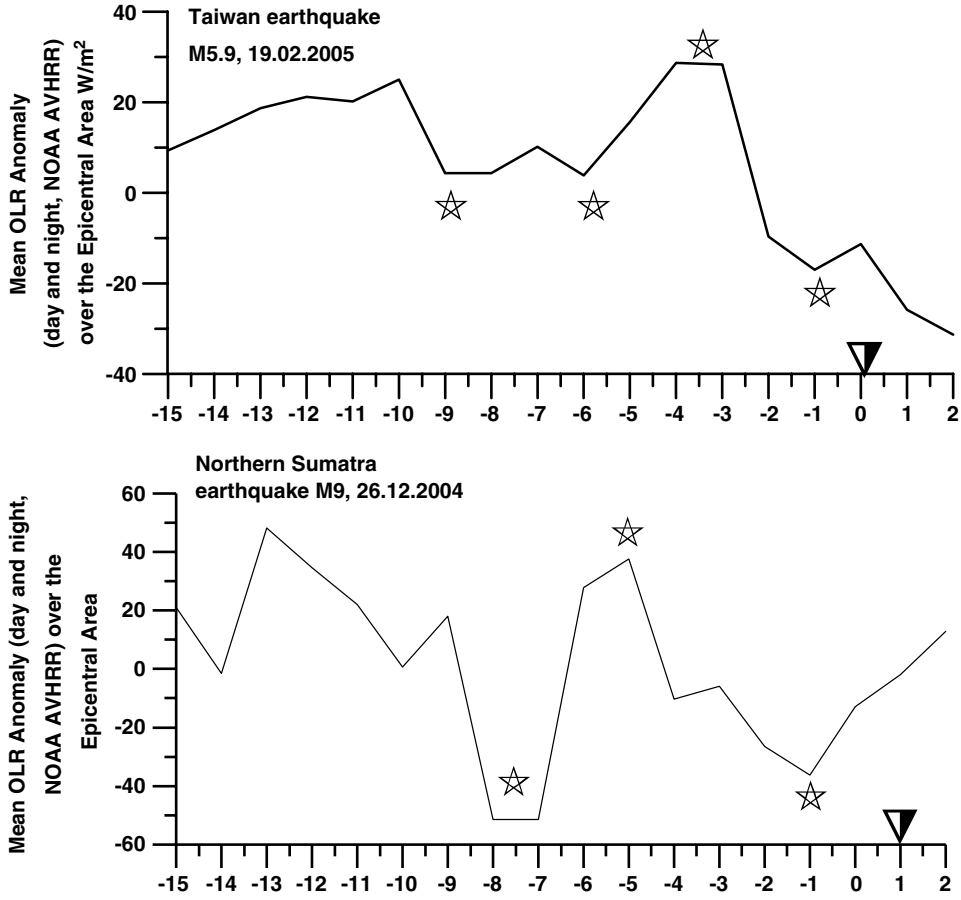

Fig. 6. Top panel – variations of ongoing longwave radiation (OLR) over the epicenter of Taiwan earthquake M5.7, February 18, 2005. Bottom panel – the same but for the Sumatra earthquake M9, December 26, 2004. (▼) indicates the earthquake moment, (☆) indicate main characteristic moments of the range variations before earthquake.

earthquakes have demonstrated that this parameter can be used as an indicator of the atmospheric anomaly probably connected with earthquake preparation process. Fig. 10 presents several examples of such calculations. The difference in the data presentation depends on the meteorological data quality (for some stations we have only the daily maxima and minima, for others – current variations) and the distance of the meteorological station from the epicenter. The second important factor is how much of land is included inside the area of the earthquake preparation (3). For example, in the case of Sumatra earthquake (Fig. 10d), when the epicenter is in the ocean, only Indonesian and Indian islands contribute in atmospheric variations through radon emanations. So regardless the very large magnitude of the earthquake (M9), the index ΔU is not so large as for the Parkfield earthquake (Fig. 10b) where both epicenter and the whole earthquake preparation area are on the land.

6. Active experiment on artificial ionization – check of the radon ionization phenomena

It is possible to produce artificial air ionization by applying high voltage to a narrow wire or to special equipment consisting of narrow needles known as "Chizhevsky chandelier" (Chizhevsky, 1960). Such instruments are widely used now in medicine for creation of negative air-ions. Depending on spatial scale and the ion current produced by the installation, different effects in the atmosphere can be caused. Pokhmelnykh (2003) made estimations showing the possibility of creation of special installation for the weather correction. The number of condensation heat P_c released in the unit column of air can be expressed as

$$P_c = m_{max} U_0 e^{-1} j_a \tag{9}$$

where e – elementary electric charge, j_a – vertical conductivity current in atmosphere.

Under condition of artificial ionization the ion production rate dN/dt can be expressed as

$$\frac{dN}{dt} = I_g e^{-1} \tag{10}$$

where I_g is the current of ion generator.

Using (2) and (9) the heat P_a released into the atmosphere can be expressed as

$$P_a = m_{max} U_0 e^{-1} I_g \tag{11}$$

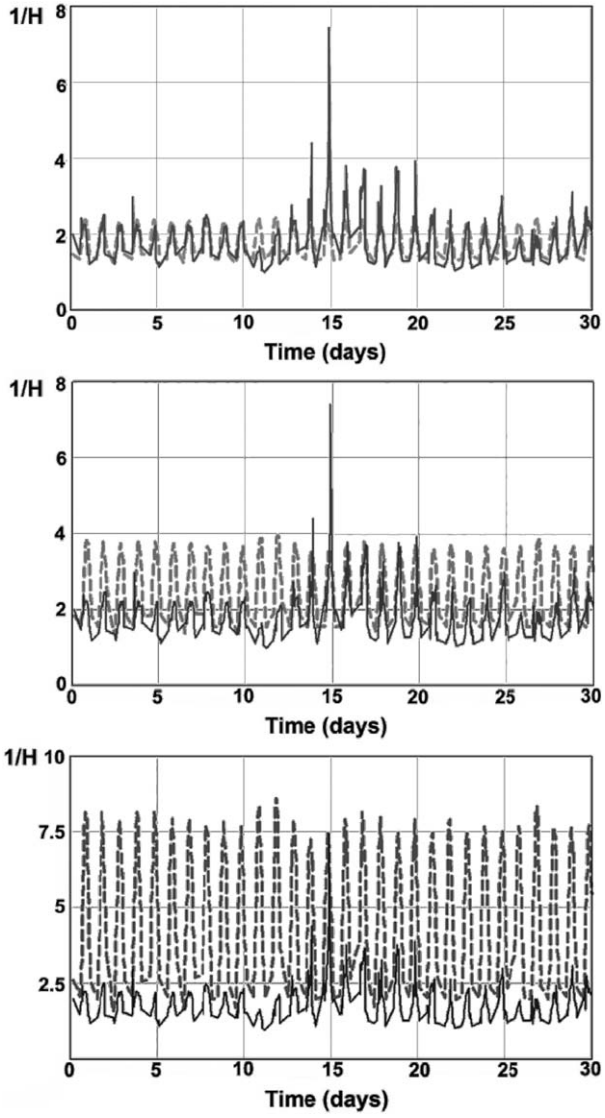

Fig. 7. Comparison of the inverse value of the experimentally measured relative humidity at Colima station (continuous line) and the inverse value of calculated relative humidity (dashed grey line). From top to bottom calculated correction of $\Delta U = 0.019$; 0.022 and 0.03 eV.

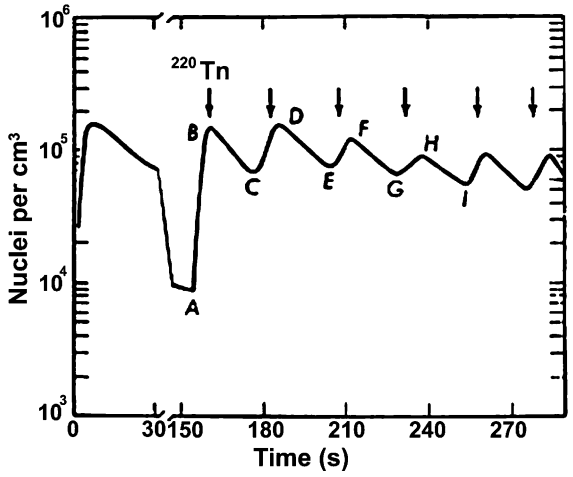

Fig. 8. Particles formed in filtered Parisian air, with the addition of regular cycles of Thoron (from Bricard et al., 1968).

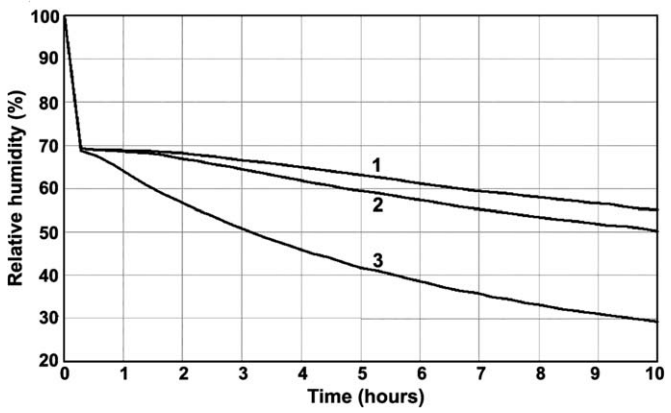

Fig. 9. Model calculations of relative humidity changes under ionization impact for the three values of the chemical potential correction $\Delta U = 0.019$ (curve 1); 0.022 (curve 2) and 0.03 eV (curve 3).

The power consumption P_g spent to produce ionization can be expressed as

$$P_g = k\frac{dN}{dt}e\varphi_i = kI_g\varphi_i \quad (12)$$

where φ_i – air ionization potential, and k is the ratio of really spent energy for the air molecule ionization to the ionization potential. It was experimentally determined that k is of order of 10^4. Therefore, the gain K_g which is in relation to the thermal energy released in the atmosphere P_a to the energy spent for ionization P_g will be

$$K_g = P_a/P_g = m_{max}U_0/ke\varphi_i \approx 5 \times 10^8 \quad (13)$$

Using these estimations the ELAT company in Mexico started experiments with installations of artificial air ionization to produce the artificial precipitation in the desert areas of Mexico. Fig. 11 demonstrates the changes of the air temperature after beginning of action of the installation of artificial ionization. It is interesting to note that the time scale of the air temperature changes is the same order (near 5 days) as of the temperature variations associated with the earthquakes (see Figs. 3, 5 and 6).

7. Discussion

The physical mechanism was proposed to explain the observed atmosphere parameters (air temperature and relative humidity) variations around the time of strong earthquakes within the earthquake preparation area. The mechanism is based on the physical and chemical processes taking place in the atmosphere as a result of action of ionizing radiation by radon gas. The ions formed as a result of ionization process and chemical reactions serve as the centers of water vapor condensation. During condensation the large amount of latent heat of evaporation is released, which leads to the changes of the air temperature. Because

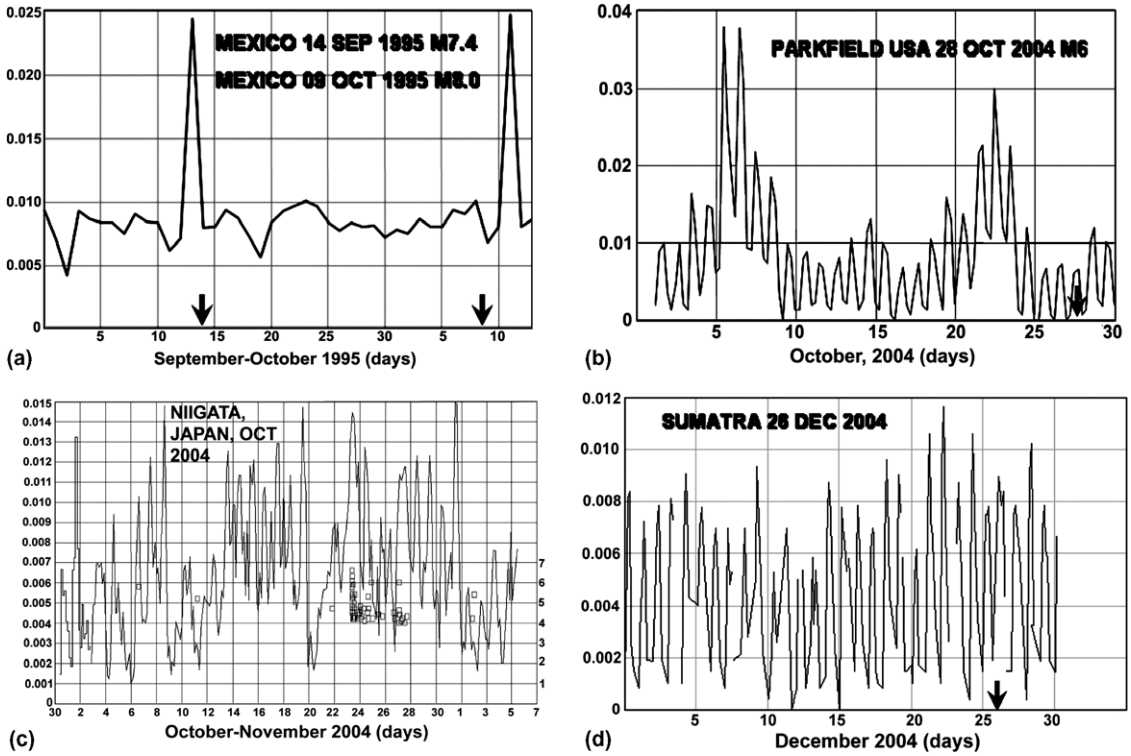

Fig. 10. Variations of the chemical potential ΔU around the time of strong earthquakes: (a) two consequent earthquake at the Pacific coast of Mexico 14 September and 09 October 1995; (b) Parkfield earthquake 28 October 2004; Niigata seismic swarm in Japan in October 2004 (the seismic shocks are indicated by squares, the earthquake magnitude is shown at right axis); Sumatra earthquake 26 December 2004. Earthquake moments are indicated by arrows.

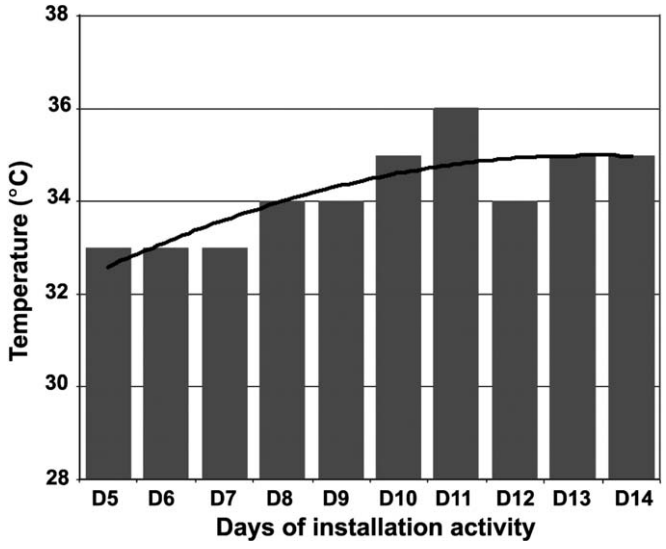

Fig. 11. The maximum daily temperature variations at the San Jose de Cabo station during period of activity of the installation for artificial air ionization. Solid line – the running average.

of condensation the air relative humidity is changing as well. The process of aerosol-size particles formation as a result of air ionization has universal character. It is observed in troposphere as a result of the cosmic rays action on the atmosphere (Yu and Turco, 2001; Timofeev et al., 2003), it was proved in the laboratory experiments (Bricard et al., 1968), it takes place under action of the radon in the near ground layer of atmosphere (Pulinets and Boyarchuk, 2004). In the case of radon, it is well known that radon emanation can be registered at any time, not just before the earthquake. It means that the all plasmachemical processes described above are not unique for earthquakes, and take place continuously. But the level of radon emanation increases before earthquakes, which leads to the deviations of the plasmachemical composition, air temperature and humidity and atmospheric electricity registered experimentally.

The observed variations are mainly due to the changes of the chemical potential of the new formed particles. We proposed a method which permits to estimate the changes of the chemical potential using the ordinary meteorological data of atmosphere parameters. For the given area it is possible to create the local model for the chemical potential ΔU and then use it in estimation of the potential danger of the approaching earthquake.

The most important thing which should be taken into account is that it is not necessary to have a powerful source of energy to produce the observable changes of the air temperature and humidity. The energy is already provided by the Sun and is stored in the water vapor in the form of the latent heat of evaporation. The ionization is the catalytic process which helps to release the stored energy.

8. Conclusion

From the theoretical considerations presented in the part 4 we can conclude that the air ionization provided by radon in the seismically active areas is responsible for the observed variations of the air temperature and humidity before strong earthquakes. The time scale of the observed variations is of order of one–two weeks before the seismic shock. In the perspective of the long time observations (several tens of years) the month of the seismic event has usually anomalously high temperature in comparison with other years.

According to the interpretation of the satellite remote sensing measurements of the infrared emission from the ground surface we can now propose rather variations of the near ground air temperature rather than the ground surface temperature as a source of observed variations.

Acknowledgements

This work was supported by the grants of PAPIIT IN 126002, CONACYT 40858-F and NASA 621-30-30-20. The authors thank the Mexican National Institute of Statistics, Geography and Informatics (INEGI) for providing the GPS data and would like to acknowledge the MODIS science Team and LP DAAC for making their data available to the user community.

References

Bricard, F., Billard, F., Madelaine, G., 1968. Formation and evolution of nuclei of condensation that appear in air initially free of aerosols. J. Geophys. Res. 54, 39–52.

Chizhevsky, A.L., 1960. Air-ionification in the national economy. Gosplanizdat, Moscow (in Russian).

Dey, S., Singh, R.P., 2003. Surface latent heat flux as an earthquake precursor. Nat. Haz. Earth Syst. Sci. 3, 749–755.

Dobrovolsky, I.R., Zubkov, S.I., Myachkin, V.I., 1979. Estimation of the size of earthquake preparation zones. Pageoph 117, 1025–1044.

Fermi, E., 1956. Thermodynamics. Dover Publications, Great Britain, 160p.

Green, H.L., Lane, W.R., 1964. Particulate Clouds: Dusts, Smokes and Mists. Spon Ltd., London, 471p.

Inan S., Researches for possible earthquake precursor(s) In the Marmara region (NW Turkey), International Workshop on Early Warning Systems for Earthquake Monitoring by Using Space Technology, Istanbul, Turkey, 1–2 February, 2005.

Mil'kis, M.R., 1986. Meteorological precursors of earthquakes Izvestiya. Earth Phys. 22, 195–204.

Ouzounov, D., Freund, F., 2004. Mid-infrared emission prior to strong earthquakes analyzed by remote sensing data. Adv. Space Res. 33, 268–273.

Ouzounov, D., Pulinets, S., 2005. Methodology and techniques for monitoring the short term ionospheric and near infrared precursory activities prior to main earthquake, (part II), International Workshop on Early Warning Systems for Earthquake Monitoring by Using Space Technology, Istanbul, Turkey, 1–2 February.

Ouzounov D., Pulinets S., Cervone G., Ciraolo L., Singh R., Kafatos M., Taylor P., 2005. Atmospheric processes in reaction of Northern Sumatra Earthquake sequence December 2004–April 2005, AGU, 86(18), Jount. Assem. Supl., Abstract U53B-01.

Ouzounov, D., Defu, L., Chun, K., Taylor, P., 2006. The outgoing long wave radiation variability prior to the major earthquake by analyzing IR satellite data. Tectonophysics 421, in press.

Pokhmelnykh, L.A., 2003. Atmosphere electricity as a manifestation of the Earth–Sun interaction with the space. Appl. Phys. 4, 34–43.

Pulinets, S.A., Boyarchuk, K.A., 2004. Ionospheric Precursors of Earthquakes. Heidelberg, Springer, Berlin, Heidelberg, 315p.

Schulz, J., Meywerk, J., Ewald, S., Schlüssel, P., 1997. Evaluation of satellite-derived latent heat flux. J. Climate 16, 2782–2795.

Sedunov, Y.S., Volnovitskii, O.A., Petrov, N.N., Reitenbakh, R.G., Smirnov, V.I., Chernikov, A.A., 1997. Atmosphere. Handbook (Reference data and Models). Gidrometeoizdat, Leningrad.

Timofeev, V.E., Grigor'ev, V.G., Morozova, V.I., Skryabin, N.G., Samsonov, S.N., 2003. Effect of cosmic rays on the latent energy of atmosphere. Geomagn. Aeron. 43, 640–646.

Tramutoli, V., DiBello, G., Pergola, N., Piscitelli, S., 2001. Robust satellite techniques for remote sensing of seismically active areas. Ann. Geofis. 44, 295–312.

Tronin, A.A., 1999. Satellite thermal survey application for earthquake prediction. In: Hayakawa, M. (Ed.), Atmospheric and Ionospheric Phenomena Associated with Earthquakes. TERRAPUB, Tokyo, pp. 717–746.

Tronin, A.A., Hayakawa, M., Molchanov, O.A., 2004. Thermal IR satellite data application for earthquake research in Japan and China. J. Geodyn. 33, 519–534.

Yavorski, B.M., Detlaf, A.A., 1996. Physics Reference Book. Nauka, Fismatlit, Moscow, 619p.

Yu, F., Turco, R.P., 2001. From molecular clusters to nanoparticles: the role of ambient ionization in tropospheric aerosol formation. J. Geophys. Res. 106 (D5), 4797–4814.

Zafrir, H., Steinitz, G., Ginzburg, B., Shirman, B., Hrvoic, I., 2005. Current achievements in the combined research of Rn emanation, earth magnetic field and the seismo-activity variations, along the Dead Sea Rift, Israel, as ground truth for space observations. In: First DEMETER Guest Investigators Workshop, CNES, Paris, France, 2–4 May 2005.

Zatsepina, G.N., 1998. The Physical Properties and Structure of Water. Moscow State University Publishing, Moscow, 184p.